Site Identification of Carboxyl Groups on Graphene Edges with Pt Derivatives

Ryota Yuge,[†,*] Minfang Zhang,[‡] Mutsumi Tomonari,[†] Tsutomu Yoshitake,[†] Sumio Iijima,[†,‡,§] and Masako Yudasaka[†,‡,*]

[†]Nano Electronics Research Laboratories, NEC Corporation, 34 Miyukigaoka, Tsukuba 305-8501, Japan, [‡]SORST, Japan Science and Technology Agency, c/o NEC Corporation, 34 Miyukigaoka, Tsukuba 305-8501, Japan, and [§]Meijo University, 1-501 Shiogamaguchi, Nagoya 468-8502, Japan

ABSTRACT Although chemical functionalization at carboxyl groups of nanocarbons has been vigorously investigated and the identities and quantities of the carboxyl groups have been well studied, the location of carboxyl groups had not previously been clarified. Here, we show that site identification of carboxyl groups is possible by using Pt−ammine complex as a stain. After Pt−ammine complexes were mixed with graphenes in ethanol, many Pt−ammine complex clusters with an average size of about 0.6 nm were found to exist at edges of graphene sheets, indicating that the carboxyl groups mainly existed at the graphene edges. These results will make it easier to add functionalities by chemical modifications for various applications of nanotubes and other nanocarbons.

KEYWORDS: carbon nanohorn · graphene · nanotube · subnanometer-sized Pt cluster

Nanocarbon materials represented by carbon nanotubes and nanographene sheets have been of great interest because of their unique structural, electrical, and mechanical properties.[1−12] Potential applications of nanocarbon materials include electronic devices, electromechanical devices, quantum wires, ultrahigh strength engineering fibers, and catalyst supports. To develop these applications, functional molecules have been attached to the carboxyl (−COOH) groups created by oxidation on nanocarbons. The existence of −COOH groups is usually confirmed using infrared absorption spectra and by temperature-programmed thermogravimetric analysis;[13−20] however, their exact locations in the nanocarbons have not been determined. It is believed that they exist at the cut edges of the graphenes and on the graphene planes; however, this has not been verified to date. We show in this study that selective staining of the −COOH groups with Pt(IV) ($Pt(NH_3)_6(OH)_4$) (Pt−ammine complexes) was possible, and the stained spots were observed by transmission electron microscopy (TEM).

RESULTS AND DISCUSSION

The nanocarbon used in this study was nanometer-sized graphene sheets prepared as follows. We first prepared spherical aggregates of single-wall carbon nanohorns (SWNHs), pseudocylindrical objects with nanometer diameters made of single graphene sheets, by CO_2 laser ablation of graphite (no metal included) at room temperature.[21,22] The laser ablation conditions were adjusted to prepare special aggregates (petal-SWNH) that contained not only SWNH but also a lot of few-graphene-sheets with petal-like forms (P-FGS),[23] as shown in Figure 1a,b. The typical P-FGS had a width of about 30−80 nm and thickness of about 1−7 nm. Next, we removed the SWNHs but retained the P-FGS by light-assisted oxidation (LAOx) using an aqueous solution of H_2O_2[24] and obtained oxidized P-FGS (P-FGSox) (Figure 1c). The edges of P-FGSox (Figure 1d) were rougher compared with those of P-FGS (Figure 1b). We reported previously that LAOx is suitable for forming abundant −COOH groups,[24] which is also seen in this study. The Fourier-transformed infrared (FT-IR) absorption spectrum of P-FGSox (Figure 2b) showed stronger peaks of oxygenated groups (~1180 and ~1560 cm^{-1}) than those of the oxygenated groups of petal-SWNH (Figure 2a). A peak at 1760 cm^{-1} of P-FGSox was assigned to the stretching of C═O groups of carboxyl groups[13−17] and other oxygenated groups such as lactones and carboxyl anhydrides[17] (Figure 2b).

P-FGSox showed a greater weight loss in a thermogravimetric analysis (TGA) and more emissions of CO (m/z = 28) and CO_2 (m/z = 44) than petal-SWNH, suggesting that P-FGSox had abundant oxygenated groups (Figure 3). It is known that −COOH decomposes and emits only CO_2 (no CO emission) below 400 °C,[16−20] which was

*Address correspondence to ryuge@frl.cl.nec.co.jp, yudasaka@frl.cl.nec.co.jp.

Received for review June 9, 2008 and accepted August 22, 2008.

Published online September 5, 2008. 10.1021/nn800352y CCC: $40.75

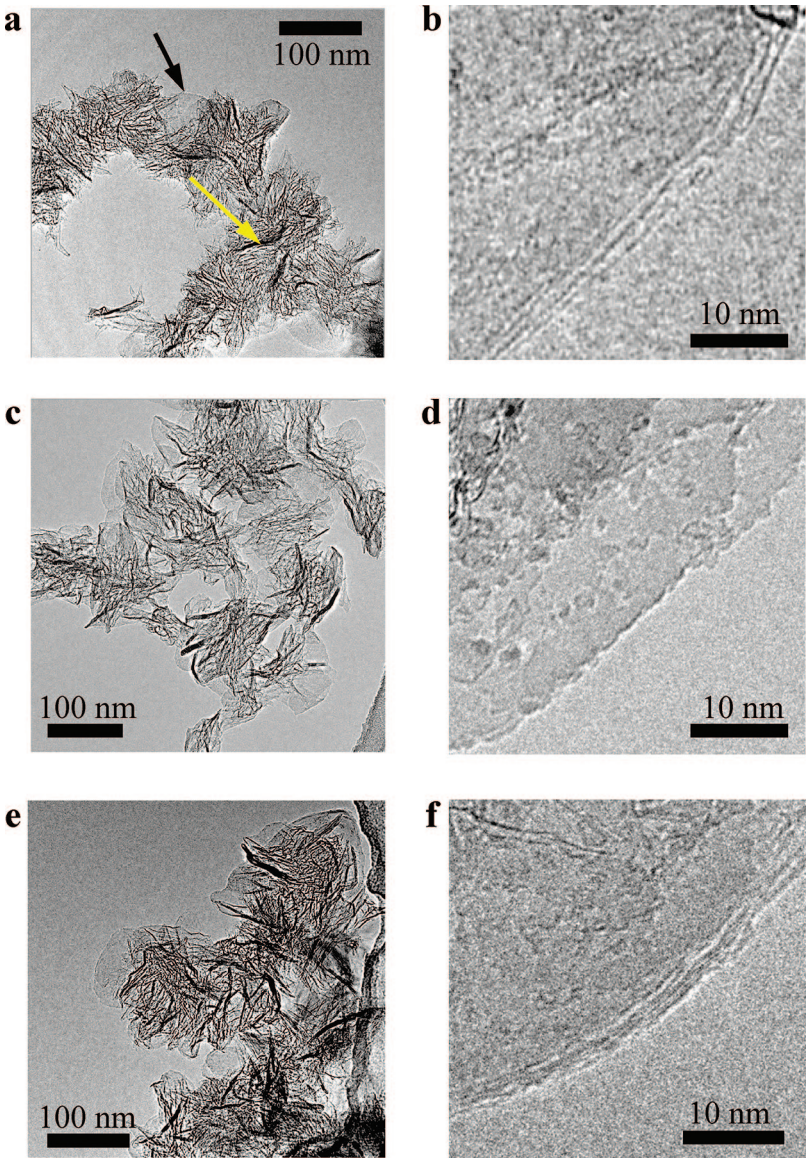

Figure 1. Typical TEM image of few-graphene-sheets with petal-like forms (P-FGS), oxidized P-FGS (P-FGSox), and heat-treated P-FGSox (HTP-FGSox). (a, b) P-FGS. The P-FGS observed from the front and side directions are indicated with black and yellow arrows, respectively (a). A magnified image shows the edges of the P-FGS (b). The darker parts of the edge lines might correspond to the bending of graphene sheets. (c, d) P-FGSox. There were more defects at the edges and more step sites in P-FGSox than in P-FGS (d). (e, f) HTP-FGSox prepared by heat treating P-FGSox to remove −COOH and other oxygenated groups. Their edges were smooth, indicating that they were thermally reconstructed (f).

observed in temperature-programmed desorption mass spectrometry (TPD-MS) of P-FGSox (red lines in Figure 3b,c). From this datum, the −COOH groups of P-FGSox are estimated to amount to about 4 wt %. At higher temperatures, the CO and/or CO_2 are believed to be emitted from carboxylic anhydrides (~500 °C)[17] and from lactones, ether, phenol, carbonyl, and/or quinone (~700 °C).[17]

Before describing the staining of the −COOH groups with hexaammine Pt(IV) ($Pt(NH_3)_6(OH)_4$) (Pt−ammine complex), we introduce a control material. We removed −COOH and other oxygenated groups from P-FGSox by heat treatment at 1200 °C in H_2 for 3 h (HTP-FGSox). No peaks corresponding to the oxygenated groups were observed in the FT-IR spectra of HTP-FGSox (Figure 2c), and a small decrease in weight was observed in TGA (Figure 3). The emission of CO_2 or CO from HTP-FGSox was not observed (blue lines in Figure 3). The TEM images of HTP-FGSox exhibited smooth graphene edges, indicating that the edges were more or less thermally annealed (Figure 1e,f).

The staining of −COOH groups of P-FGSox by the Pt−ammine complex (Pt complex/P-FGSox) was observed using a TEM. In the TEM images, many dark spots of Pt−ammine complexes at the edges and steps of P-FGSox were observed; typical spots are indicated with arrows in Figure 4a,b. The spot size distribution exhibited a maximum at 0.6 nm (Figure 4a). These Pt−ammine complex clusters were also observed as dark spots in scanning transmission electron microscopy (STEM) (Figure 4b) or as bright spots in a *Z*-contrast image (Figure 4c). (In a *Z*-contrast image, the image contrast is proportional to the square of the atomic number; therefore, the Pt atoms appear as bright spots.) Elemental analysis using energy-dispersive X-ray (EDX) spectroscopy for a selected area of about 0.25 nm^2 showed that the bright spot contained Pt (Figure 4d orange arrow); however, the featureless surface did not show such spots (Figure 4e pale-blue arrow). Therefore, we can be sure that the Pt complex preferentially attached to the edges and steps of P-FGSox and not on the featureless surface of graphene.

Interaction of −COOH of P-FGSox and the Pt−ammine complex was studied with the IR spectra. After the Pt−ammine complex deposition on P-FGSox, the IR peaks of the NH_3 group (Figure 5a green arrows) newly appeared; however, the −C═O peaks (1730 cm^{-1}) of P-FGSox became weaker (*cf.* Figure 5a red and green lines), suggesting that −COOH formed amide bonds[24,25] or ionic bonds[26,27] with the NH_3 groups. Since the −C═O peaks of such amide bonds and ionic bonds usually appear in a wavenumber region of 1550−1650 cm^{-1}, we believe that the −C═O peaks of −COOH of P-FGSox were red-shifted by forming amide bonds or ionic bonds with NH_3 groups of the Pt−ammine complex and overlapped the absorption bands of P-FGSox appearing at about 1560 cm^{-1}.

After washing Pt complex/P-FGSox with water, the NH_3 peaks became a little weaker, while the −C═O peak intensity increased to some extent (Figure 5a

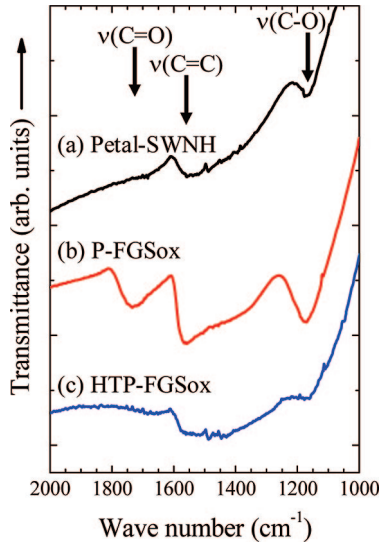

Figure 2. Analysis of oxygen-containing functional groups by FT-IR absorption spectroscopy. (a) Starting petal-SWNH, (b) P-FGSox, (c) HTP-FGSox. Assignments of the major peaks are indicated with arrows.

purple line). We presume that the −C═O with its intensity recovered by washing with water was −C═O of −COOH that ionically bonded to the NH_3 groups. The −C═O with its peak intensity not recovered was that of the amide bond.

To identify the dominant of the two types of bonds, we washed Pt complex/P-FGSox with water and found that many particles of the Pt−ammine complex washed away, as seen in the TEM image of Figure 5b. The TGA results showed that the residue quantity at 1000 °C decreased from about 15 to 8 wt % by washing with water (not shown). We consider

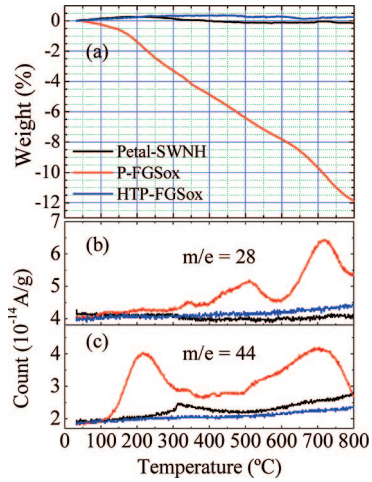

Figure 3. TGA and TPD-MS spectra of starting petal-SWNH, P-FGSox, and HTP-FGSox. (a) TGA results indicated that P-FGSox exhibited a larger weight loss than the starting aggregates and HTP-FGSox. The weight loss of P-FGSox was mainly due to thermal degradation of the oxygenated groups. (b) TPD-MS of m/z = 28 (CO) and m/z = 44 (CO_2) indicated that CO and CO_2 were emitted vigorously from the P-FGSox, but not from the starting aggregate or HTP-FGSox.

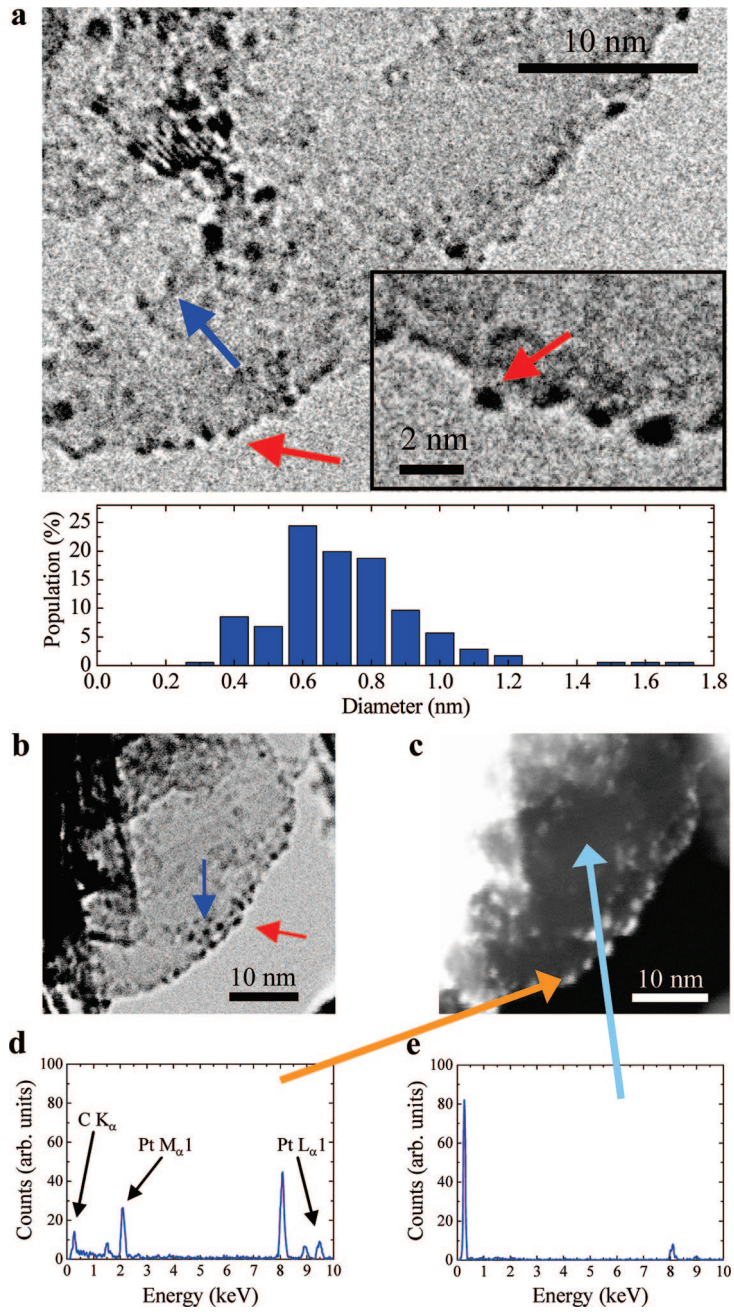

Figure 4. Preferential adsorption of Pt−ammine complexes at the edges and steps of P-FGSox. (a) TEM images of Pt complex/P-FGSox and their size distributions obtained from about 300 black spots observed in the TEM images. Pt complex clusters attached to the edges (red arrow) and steps (blue arrow). STEM (b) and *Z*-contrast (c) images of Pt complex/P-FGSox. EDX spectrum of Pt complex/P-FGSox at a bright spot indicated with an orange arrow (d) and at an area on the featureless surface pointed with a pale-blue arrow (e) in the *Z*-contrast image. In EDX spectrum (d), the peaks originating from C, K, Pt M1, and Pt L1 are indicated. The other peaks are associated with Cu and Al of the Cu grid disk (TEM sample holder) or detector bodies of the EDX analyzer.

that the Pt−ammine complex corresponding to the "8 wt %" conjugated with P-FGSox through amide bonds and the other Pt−ammine complex that was washed away with water were either ionically bonded to P-FGSox or self-aggregated, making large particles with sizes of several tens of nanometers, which we occasionally found with TEM.

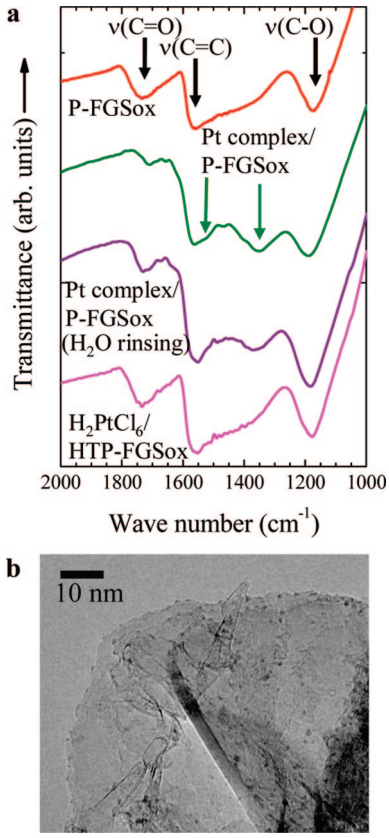

Figure 5. NH_3−COOH specific bonds. (a) FT-IR spectra of P-FGSox, Pt complex/P-FGSox, H_2PtCl_6/P-FGSox, and Pt complex/P-FGSox (H_2O rinsing). Two distinct peaks at 1370 and 1565 cm^{-1} characteristic of NH_3 moieties of the Pt−ammine complex[29] are clearly visible (green arrows). (b) TEM images of Pt complex/P-FGSox showing a smaller number of black spots of Pt−ammine complex at the edges and steps of P-FGSox after being washed with water.

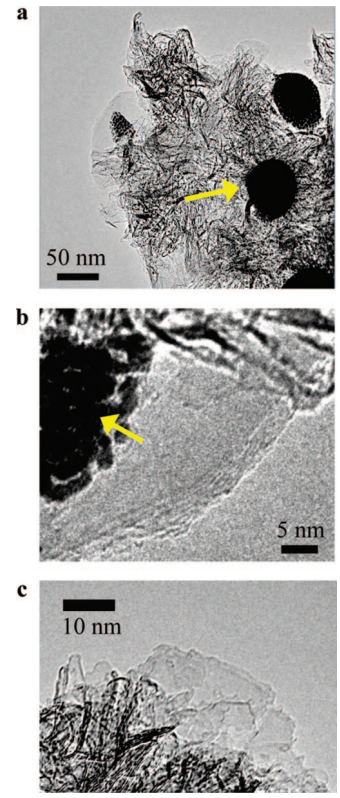

Figure 6. TEM images of HTP-FGSox with either amine or −COOH absent. (a, b) TEM images of Pt−ammine complex adsorbed on HTP-FGSox. Pt complexes formed large particles; a typical one is indicated with yellow arrows. (c) TEM image of H_2PtCl_6/P-FGSox. Almost no H_2PtCl_6 particles were found.

Concerning the interactions of −COOH of P-FGSox and Pt−ammine complex, it is alternatively presumed that the hydrogen bond was formed between −C═O and NH_3 groups that made the −C═O absorption peak red shift from 1730 to 1720 cm^{-1}.[28] In this explanation, a very small peak at 1660 cm^{-1} could be assigned to the absorption peak of −C═O that ionically interacted with NH_3 groups. However, these assignments have problems that the peak intensity became considerably small after the Pt−ammine complex was attached (Figure 5a). Thus we consider that this alternative assignment is not reasonable.

The attachment of the Pt−ammine complex to −COOH was specific because the Pt−ammine complex did not attach to the edges and steps of HTP-FGSox (Figure 1e,f) where there were no −COOH groups (Figure 2c). TEM observation of the Pt−ammine complex supported on HTP-FGSox (Figure 6a,b) did not exhibit any subnanometer-sized clusters of Pt−ammine complex attached to the edges and steps of graphenes; however, clusters with sizes of 10−50 nm were observed. On HTP-FGSox surfaces, the Pt complexes preferred to self-aggregate and form large aggregates.

We tried to load a different Pt complex (H_2PtCl_6) that does not have NH_3 groups onto P-FGSox (H_2PtCl_6/P-FGSox). The FT-IR spectrum showed no change for C═O bands (*cf.* Figure 5a red and magenta lines), and TEM observation showed few Pt clusters deposited on P-FGSox (Figure 6c).

The number of Pt−ammine complexes in the cluster observed in the microscopy images of Pt complex/P-FGSox (Figure 4) is determined as follows. Since the molecular size of the Pt−ammine complex is about 0.6 nm,[30] most of the clusters might correspond to an individual Pt−ammine complex (Figure 4), or the more likely possibility is that the Pt−ammine complexes were destroyed by the electron beam and only Pt atoms remained; in this case, the 0.6 nm cluster would contain several Pt atoms. Referring to the Pt crystal (face-centered cubic symmetry, four Pt atoms in a unit cell) lattice constant, 0.39 nm, the 0.6 nm cluster would contain about seven Pt atoms.

CONCLUSIONS

We showed that the −COOH groups were selectively stained with Pt−ammine complexes, and the locations of −COOH are identified by observing the Pt−ammine complexes with electron microscopy. Since this staining is easy, this method is invaluable for identifying the sites of the −COOH groups in nanocarbon materials. Such site

identification makes it possible to design chemical modifications and, therefore, accelerate the development of applications of nanocarbon materials such as carbon nanotubes, SWNHs, and nanographenes.

MATERIALS AND METHODS

The combustion of the petal-SWNH aggregate composed of SWNH and P-FGS (40 mg) by LAOx[24] was performed with 30% aqueous solution of H_2O_2 (100 mL) for 6 h at 100 °C under light irradiation using a Xe lamp (wavelength = 250−2000 nm, intensity = 3 W, diameter = 1 cm). The specimen was subsequently washed with pure water, followed by drying for 24 h in vacuum at 80 °C, and P-FGSox was obtained.

Pt complex/P-FGSox was prepared by dispersing P-FGSox (15 mg) in an ethanol (10 mL) solution of Pt−ammine complex (Tanaka Kikinzoku Kogyo K. K.) (0.3 mL), stirred for 12 h at room temperature, and separated from ethanol by filtration, followed by washing with ethanol and drying for 24 h in vacuum at 50 °C.[31] To remove the Pt−ammine complex bonded ionically or self-aggregated, Pt complex/P-FGSox was dispersed in 50 mL of water, sonicated for 1 min, separated from water by filtration, and washed three times with water (50 mL).

To remove the oxygenated groups and obtain HTP-FGSox, P-FGSox was heat-treated at 1200 °C in a hydrogen atmosphere (760 Torr).[32] The Pt−ammine complex was loaded on HTP-FGSox with the same method as described above. To confirm the selective adsorption of the Pt−ammine complex to −COOH groups, we put H_2PtCl_6, which is not reactive with −COOH, on P-FGSox following the same method described above for Pt−ammine complex and obtained H_2PtCl_6/P-FGSox.

The structures of the specimens were observed by TEM using a Topcon 002B with an accelerating voltage of 120 kV. FT-IR absorption spectra were measured in the transmittance mode (Perkin-Elmer spectrum). The spectrometer was purged with dry nitrogen. The spectra were recorded at a resolution of 4 cm^{-1} in the 1000−2000 cm^{-1} region. For the FT-IR measurement, the specimens were dispersed in ethanol and sprayed on ZnSe substrate. The FT-IR spectra were normalized by the transmittance at 2000 cm^{-1}. The quantity of −COOH groups on P-FGSox was estimated by TGA (TGA2950, TA Instruments) performed in a helium atmosphere at temperatures ranging from room temperature to 800 °C at a ramp rate of 5 °C/min. A constant amount (*ca.* 5 mg) of sample was used for TGA. The gas components evolved at an elevated temperature under a helium flow (50 cm^3 min^{-1}) were analyzed using TPD-MS (Rigaku Thermoplus). The existence of Pt in the Pt complex/P-FGSox was checked with STEM (Hitachi HD2300) operated at an accelerating voltage of 120 kV, equipped with an EDX analyzer. The quantity of Pt on P-FGSox was estimated by TGA performed in an oxygen atmosphere at temperatures ranging from 100 to 1000 °C at a ramp rate of 10 °C/min. A constant amount (*ca.* 2 mg) of sample was used for the TGA.

Acknowledgment. This work was in part performed under the management of the Nano Carbon Technology project supported by NEDO.

REFERENCES AND NOTES

1. Iijima, S. Helical Microtubules of Graphitic Carbon. *Nature* **1991**, *354*, 56–58.
2. Iijima, S.; Ichihashi, T. Single-Shell Carbon Nanotubes of 1-nm Diameter. *Nature* **1993**, *363*, 603–605.
3. Frank, S.; Poncharal, P.; Wang, Z. L.; Heer, W. A. Carbon Nanotube Quantum Resistors. *Science* **1998**, *280*, 1744–1746.
4. Chopra, N. G.; Benedict, L. X.; Crespi, V. H.; Cohen, M. L.; Louie, S. G.; Zettl, A. Fully Collapsed Carbon Nanotubes. *Nature* **1995**, *377*, 135–138.
5. Novoselov, K. S.; Geim, A. K.; Morozov, S. V.; Jiang, D.; Zhang, Y.; Dubonos, S. V.; Grigorieva, I. V.; Firsov, A. A. Electric Field Effect in Atomically Thin Carbon Films. *Science* **2004**, *306*, 666–669.
6. Heersche, H. B.; Jarillo-Herrero, P.; Oostinga, J. B.; Vandersypen, L. M. K.; Morpurgo, A. F. Bipolar Supercurrent in Graphene. *Nature* **2007**, *446*, 56–59.
7. Kim, P.; Lieber, C. M. Nanotube Nanotweezers. *Science* **1999**, *286*, 2148–2150.
8. Wei, B. Q.; Vajtai, R.; Jung, Y.; Ward, J.; Zhang, R.; Ramanath, G.; Ajayan, P. M. Assembly of Highly Organized Carbon Nanotube Architectures by Chemical Vapor Deposition. *Chem. Mater.* **2003**, *15*, 1598–1606.
9. Thess, A.; Lee, R.; Nikolaev, P.; Dai, H.; Petit, P.; Robert, J.; Xu, C.; Lee, Y. H.; Kim, S. G.; Rinzler, A. G. *et. al.* Crystalline Ropes of Metallic Carbon Nanotubes. *Science***1996**, *273*, 483−487.
10. Vigolo, B.; Pénicaud, A.; Coulon, C.; Sauder, C.; Pailler, R.; Journet, C.; Bernier, P.; Poulin, P. Macroscopic Fibers and Ribbons of Oriented Carbon Nanotubes. *Science* **2000**, *290*, 1331–1334.
11. Hull, R. V.; Li, L.; Xing, Y.; Chusuei, C. C. Pt Nanoparticle Binding on Functionalized Multiwalled Carbon Nanotubes. *Chem. Mater.* **2006**, *18*, 1780–1788.
12. Chen, J.; Wang, M.; Liu, B.; Fan, Z.; Cui, K.; Kuang, Y. Platinum Catalysts Prepared with Functional Carbon Nanotube Defects and Its Improved Catalytic Performance for Methanol Oxidation. *J. Phys. Chem. B* **2006**, *110*, 11775–11779.
13. Chen, J.; Hamon, M. A.; Hu, H.; Chen, Y.; Rao, A. M.; Eklund, P. C.; Haddon, R. C. Solution Properties of Single-Walled Carbon Nanotubes. *Science* **1998**, *282*, 95–98.
14. Kim, U. J.; Furtado, C. A.; Liu, X.; Chen, G.; Eklund, P. C. Raman and IR Spectroscopy of Chemically Processed Single-Wall Carbon Nanotubes. *J. Am. Chem. Soc.* **2005**, *127*, 15437–15445.
15. Zhang, J.; Zou, H.; Qing, Q.; Yang, Y.; Li, Q.; Liu, Z.; Guo, X.; Du, Z. Effect of Chemical Oxidation on The Structure of Single-Walled Carbon Nanotubes. *J. Phys. Chem. B* **2003**, *107*, 3712–3718.
16. Kuznetsova, A.; Mawhinney, D. B.; Naumenko, V.; Yates, J. T., Jr.; Liu, J.; Smalley, R. E. Enhancement of Adsorption Inside of Singe-Walled Nanotubes: Opening the Entry Ports. *Chem. Phys. Lett.* **2000**, *321*, 292–296.
17. Figueiredo, J. L.; Pereira, M. F. R.; Freitas, M. M. A.; Orfao, J. J. M. Modification of the Surface Chemistry of Activated Carbons. *Carbon* **1999**, *37*, 1379–1389.
18. Vix-Guterl, C.; Couzi, M.; Dentzer, J.; Trinquecoste, M.; Delhaes, P. Surface Characterizations of Carbon Multiwall Nanotubes: Comparison between Surface Active Sites and Raman Spectroscopy. *J. Phys. Chem. B* **2004**, *108*, 19361–19367.
19. Zhuang, Q.-L.; Kyotani, T.; Tomita, A. The Change of TPD Pattern of O_2-Gasified Carbon upon Air Exposure. *Carbon* **1994**, 539–540.
20. Otake, Y.; Jenkins, R. G. Characterization of Oxygen-Containing Surface Complexes Created on a Microporous Carbon by Air and Nitric Acid Treatment. *Carbon* **1993**, *31*, 109–121.
21. Iijima, S.; Yudasaka, M.; Yamada, R.; Bandow, S.; Suenaga, K.; Kokai, F.; Takahashi, K. Nano-Aggregates of Single-Walled Graphitic Carbon Nano-Horns. *Chem. Phys. Lett.* **1999**, *309*, 165–170.
22. Iijima, S. Carbon Nanotubes: Past, Present, and Future. *Physica B* **2002**, *323*, 1–5.
23. Azami, T.; Kasuya, D.; Yuge, R.; Yudasaka, M.; Iijima, S.; Yoshitake, T.; Kubo, Y. Large-Scale Production of Single-Wall Carbon Nanohorns with High Purity. *J. Phys. Chem. C* **2008**, *112*, 1330–1334.
24. Zhang, M.; Yudasaka, M.; Ajima, K.; Miyawaki, J.; Iijima, S. Light-Assisted Oxidation of Single-Wall Carbon Nanohorns for Abundant Creation of Oxygenated Groups That Enable

Chemical Modifications with Proteins To Enhance Biocompatibility. *ACS Nano* **2007**, *1*, 265–272.
25. Hamon, M. A.; Chen, J.; Hu, H.; Chen, Y.; Itkis, M. E.; Rao, A. M.; Eklund, P. C.; Haddon, R. C. Dissolution of Single-Walled Carbon Nanotubes. *Adv. Mater.* **1999**, *11*, 834–840.
26. Fiorilli, S.; Onida, B.; Bonelli, B.; Garrone, E. *In Situ* Infrared Study of SBA-15 Functionalized with Carboxylic Groups Incorporated by A Co-Condensation Route. *J. Phys. Chem. B* **2005**, *109*, 16725–16729.
27. Zhao, W.; Song, C.; Pehrsson, P. E. Water-Soluble and Optically pH-Sensitive Single-Walled Carbon Nanotubes from Surface Modification. *J. Am. Chem. Soc.* **2002**, *124*, 12418–12419.
28. Piao, L.; Liu, Q.; Li, Y.; Wang, C. Adsorption of L-Phenylalanine on Single-Wall Carbon Nanotubes. *J. Phys. Chem. C* **2008**, *112*, 2857–2863.
29. Nakamoto, K. Infrared and Raman Spectra of Inorganic and Coordination Compounds, 3rd ed.; Wiley: New York, 1978; pp 197−202.
30. Tomonari, M., unpublished. The geometry of hexaammine Pt(IV) ($Pt(NH_3)_6(OH)_2$) was optimized by B3LYP/6-31G(d).
31. Murata, K.; Yudasaka, M.; Iijima, S. Hydrogen Production from Methane and Water at Low Temperature Using EuPt Supported on Single-Wall Carbon Nanohorns. *Carbon* **2006**, *44*, 818–820.
32. Miyawaki, J.; Yudasaka, M.; Iijima, S. Solvent Effects on Hole-Edge Structure for Single-Wall Carbon Nanotubes and Single-Wall Carbon Nanohorns. *J. Phys. Chem. B* **2004**, *108*, 10732–10735.